한국압력기기공학회 논문집
제7권 제1호 2011년 3월 pp. 1－8

신형안전주입탱크의 성능개선 및 검증

윤영중* · 주인철† · 권태순* · 송철화*

Performance Improvement and Validation of Advanced Safety Injection Tanks

Young Jung Youn*, In-Cheol Chu†, Tae-Soon Kwon* and Chul-Hwa Song*

(Received 20 DEC 2010, Accepted 20 JAN 2011)

ABSTRACT

Advanced SITs of the evolutionary PWRs have the advantage that they can passively control the ECC water discharge flow rate. Thus, the LPSI pumps can be eliminated from the safety injection system owing to the benefit of the advanced SITs. In the present study, a passive sealing plate was designed in order to overcome the shortcoming of the advanced SITs, i.e., the early nitrogen discharge through the stand pipe. The operating principle of the sealing plate depends only on the natural phenomena of buoyancy and gravity. The performance of the sealing plate was evaluated using the VAPER test facility, equipped with a full-scale SIT. It was verified that the passive sealing plate effectively prevented the air discharge during the entire duration of the ECC water discharge. Also, the major performance parameters of the advanced SIT were not changed with the installation of the sealing plate.

Key Words : Passive sealing plate(피동 밀폐판), Fluidic device(피동유량조절기구), Safety injection tank(안전주입탱크), APR1400(신형경수로), VAPER(밸브성능평가시험시설), Full-scale performance verification (실규모 성능검증)

Nomenclature

A = cross-sectional area (m^2)
g = gravitational acceleration constant (m^2/s)
h = ECC water level (m)
K = pressure loss coefficient (-)
P = pressure (Pa)
Q = volumetric flow rate (m^3/s)
t = time (sec)
v = mean velocity (m/s)
V = volume (m^3)
W = mass flow rate (kg/s)
Δh = ECC water level difference (m)
ΔP = pressure difference (Pa)
Δt = time difference (sec)
ρ = density (kg/ m^3)

Subscript
air = air in SIT
ECC = ECC water
FD = Fluidic Device
pipe = discharge pipe
SIT = safety injection tank

† 주인철, 회원, 한국원자력연구원
E-mail : chuic@kaeri.re.kr
TEL : (042)868-2845 FAX : (042)861-6438
* 한국원자력연구원

1. Introduction

Evolutionary type next generation nuclear power

reactors have been developed since the 1980's. One of the characteristics of these new reactors is an independence among safety injection systems (SISs) and an adoption of passive components. The passive components decrease the complexity of SIS and improve the reliability of the system.

Some evolutionary type PWRs such as APR1400 and APWR adopt an advanced safety injection tank (SIT). For example, the SIT of APR1400 has a fluidic device which passively controls ECC (Emergency Core Cooling) water injection flow rate into reactor coolant system during refill and reflood phases of LB-LOCA (i.e., a high injection flow rate during the refill phase and a low injection flow rate during the reflood phase).

The benefit of the fluidic device is the elimination of the function of low pressure safety injection (LPSI) pump from the safety injection system (Fig. 1). Conventional nuclear power plants were designed to deliver ECC water into a reactor vessel by SITs in the blowdown and refill phases, and to deliver the ECC water by safety injection pumps during the reflood phase in the event of LB-LOCA (Large Break Loss of Cooling Accident) (Fig. 1). The SIT of the conventional nuclear power plant delivers excessive ECC water to the reactor vessel after the water level has been raised

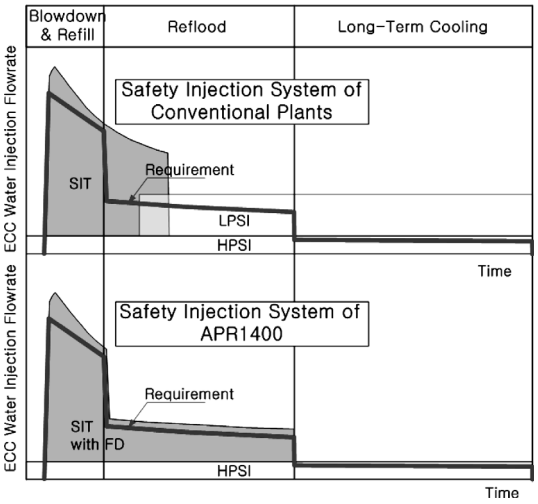

Fig. 1 Role of the safety injection system components of a conventional nuclear power plant and APR1400

to the cold leg bottom elevation, causing ECC water to flow into containment.

APR1400 is scheduled to be in commercial operation by the mid 2010s in Korea. APR1400 has adopted new design features as well as raising power capacity to 1400MWe[1]. The new design features include four mechanically independent trains for the safety injection system with a DVI (Direct Vessel Injection) mode. Each train of safety injection system consists of a safety injection pump and a passively operating SIT. KAERI (Korea Atomic Energy Research Institute) has performed various thermal hydraulic tests to evaluate and validate the performance of these new APR1400 design features[2].

The vortex device using the vortex flow effect was invented in 1928 by Thoma[3]. The concept of an advanced accumulator that employs a vortex flow control device (vortex damper) was developed by Mitsubishi Heavy Industries, Ltd. (MHI). It functions by switching the ECC water discharge flow rate during the refill and the reflood phases. Experiments were carried out with 1/5 scale and 1/3 scale test rigs[4]. A design verification test for the advanced accumulator of the Japanese advanced PWR with a 1/2 scale test rig (i.e., full height of 9m and 1/2 scaled diameter of 2m) was carried out[5]. Here, the peak discharge flow rate was about 300kg/s under actual pressure conditions. KAERI has developed and evaluated the flow controlling performance of the advanced SIT of the APR1400 using a prototypical full-scale test facility, called VAPER (Valve Performance Evaluation Rig), and the performance of the APR1400 SIT satisfied major design and licensing requirements[6].

However, one shortcoming of such advanced SIT (or accumulator) is that the nitrogen gas in the upper part of the SIT starts to be discharged before the ECC water in the SIT is depleted, which could increase an uncertainty in a safety analysis results for LB-LOCA.

A new passive device was designed to prevent the early discharge of the nitrogen gas and its performance was evaluated using the full scale test facility, VAPER, in this study.

2. Flow Controlling Mechanism of the Advanced Safety Injection Tanks

Explanation will be given focusing on the APR1400 SIT because the flow controlling mechanisms of APWR accumulator and APR1400 SIT are similar. Construction of the APR1400 passive flow controlling SIT and the fluidic device are presented in Fig. 2. Flow structures inside the vortex chamber are illustrated in Fig. 3.

ECC water that is delivered through the supply port flows into the vortex chamber through supply nozzles (Fig. 3). On the other hand, the ECC water that is delivered through the four control ports flows into the vortex chamber through control nozzles (Fig. 3). Finally, the ECC water is discharged through an exit port at the bottom center of the vortex chamber.

Control nozzles inject ECC water tangentially into the vortex chamber, establishing a strong swirling flow inside the vortex chamber when ECC water is only injected through the control nozzles (Fig. 3 (b)). This causes a high flow resistance through the fluidic device. In contrast to the control nozzle, each supply nozzle has some angle with a neighboring control nozzle in order to minimize the swirling flow effect (Fig. 3 (a)). Consequently, the flow resistance through the fluidic device becomes significantly decreased when ECC water is delivered into the vortex chamber through both the supply and control nozzles.

ECC water is delivered into the vortex chamber through both the supply and control nozzles at the early stage of LB-LOCA when the SIT starts to operate. The SIT provides a high discharge flow rate of ECC water which is required during the refill phase of LB-LOCA. When the ECC water level is lowered to below the top of the stand pipe, the flow path via the supply nozzle is absent and all ECC water is delivered only through the control nozzle. As a result, the discharge flow rate of ECC water is decreased, but is still sufficient to remove decay heat during the reflood phase, extending the total duration of ECC water injection.

As mentioned, the ECC water is delivered only through the control nozzles when the ECC water level is below the top of the stand pipe, which makes the water level in the stand pipe lower than the water level in the SIT due to the pressure drop through the control

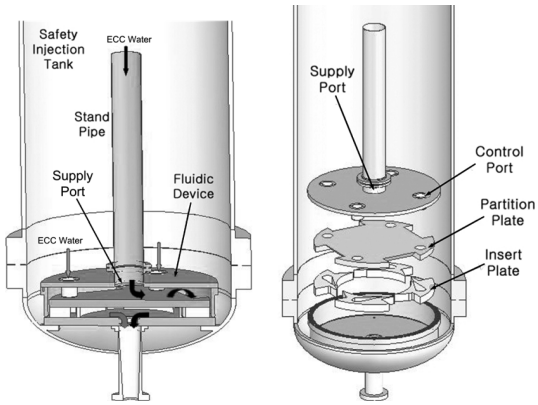

Fig. 2 Structures of the passive flow controlling safety injection tank and the fluidic device

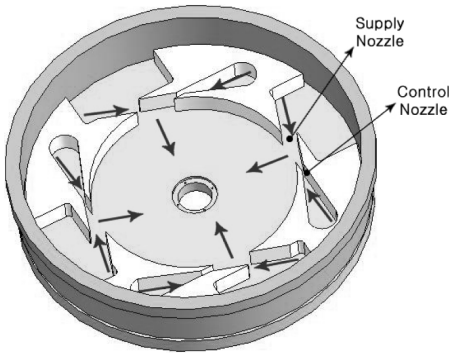

(a)

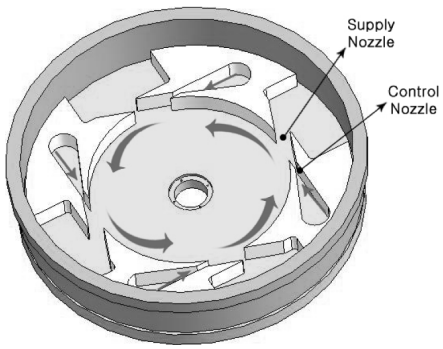

(b)

Fig. 3 Illustration of a typical flow structure inside the vortex chamber : (a) high flow rate condition, (b) low flow rate condition

nozzle. This results in the earlier depletion of the ECC water in the stand pipe and the discharge of the nitrogen gas occurs through the empty stand pipe before the ECC water in the SIT is depleted.

3. Design and Working Principle of the Passive Sealing Plate

The sealing plate moves up and down along the guide rods using the natural phenomena of buoyancy and gravity (Fig. 4). The sealing plate can be made of the materials with the density lower than the ECC water. Polyethylene can be a good candidate because its density (about 925kg/m^3) is lower than ECC water, and it has sufficiently good corrosion resistance and fracture toughness.

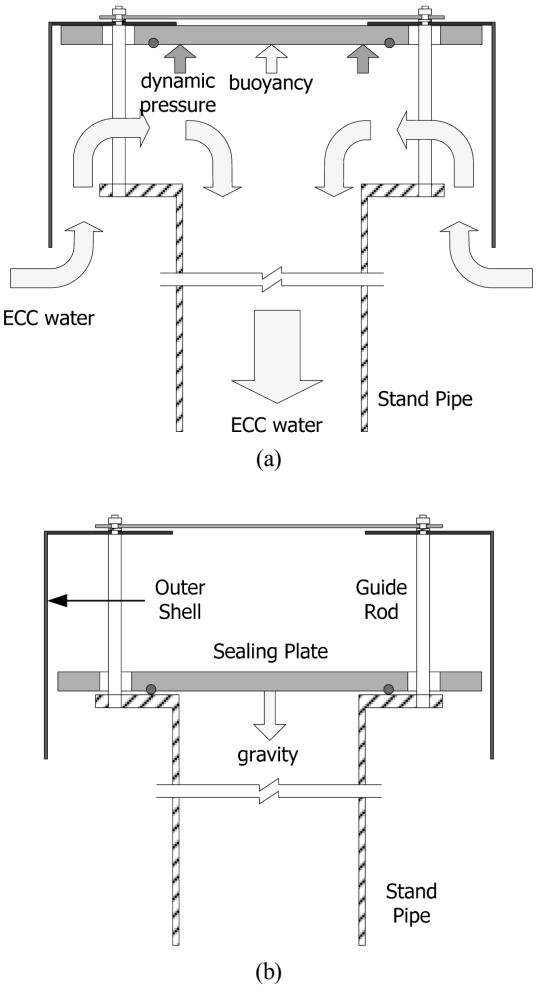

Fig. 4 Working principle of the sealing plate : (a) floating due to buoyancy and dynamic pressure, (b) falling down due to gravity

The sealing plate always floats above the stand pipe due to the density difference between the plate and the ECC water when the SIT is filled with the ECC water. The outer shell changes the direction of the ECC water flow into vertical upward direction before it enters inside the outer shell, which transfers the dynamic pressure to the sealing plate in upward direction thus resulting in the additional floating force.

When the ECC water level is lowered to below the top of the stand pipe, the sealing plate falls down due to the gravity and closes the stand pipe inlet. Therefore, the discharge of the nitrogen gas through the stand pipe is prevented with the installation of the sealing plate.

4. Experimental Verification

4.1 Experimental Facility

The performance of the sealing plate was verified using the VAPER test facility which was constructed to evaluate the performance of APR1400 advanced SIT. Unborated de-mineralized water and compressed air were used instead of borated ECC water and nitrogen gas, respectively, in this study.

The SIT has an inner diameter of 2.74m, a height of 11.95m, and a volume of 68.13m^3, which is the same geometrical shape and size as the prototype SIT of APR1400. The SIT was pressurized up to 4.0 MPa by the compressed air supply system. ECC water discharged from the SIT flowed into the water storage tank which had a volume of 97m^3. The tank was kept at one atmospheric pressure during the experiments (Fig. 5). The fluidic device in the present experiments was modified from the fluidic device of the APR1400 SIT in order to make the discharge of the nitrogen gas start ealier. The inner diameter and height of the stand pipe was 0.39m and 3.1m, respectively.

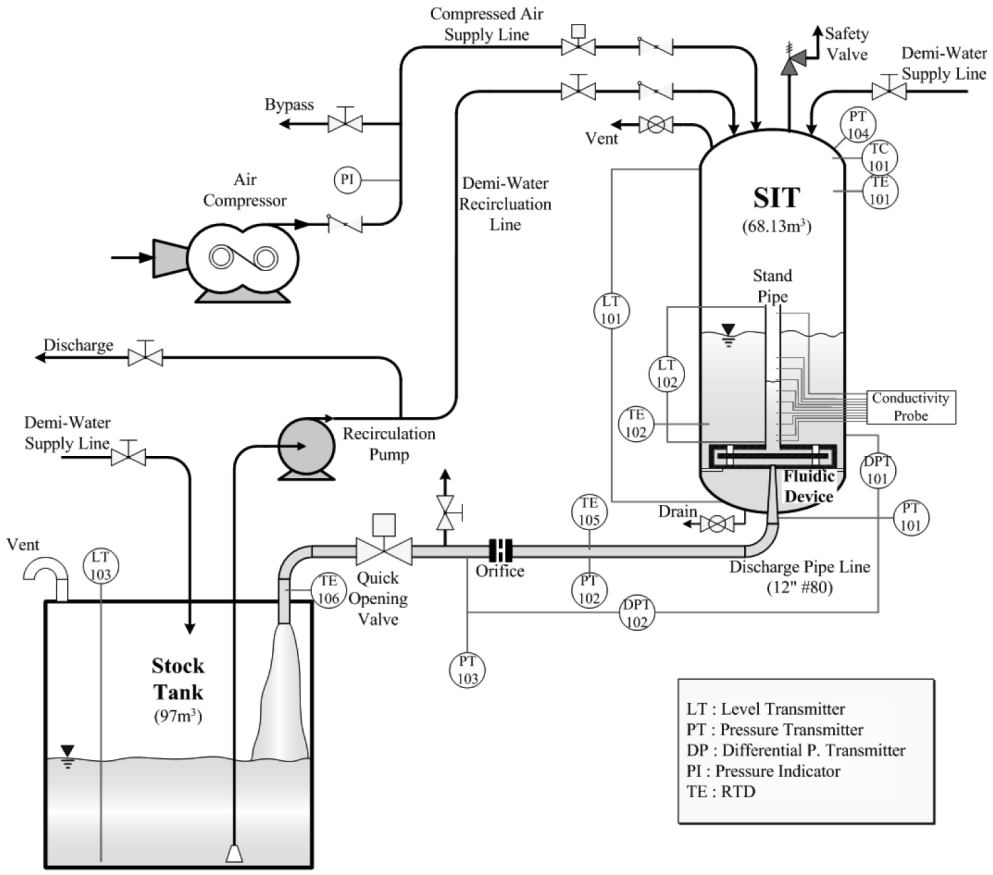

Fig. 5 Schematic of the full-scale test facility, VAPER

4.2 Experimental Condition

Two tests were carried out in order to validate the performance of the sealing plate for the same fluidic device under the similar conditions of SIT level and pressure. One test was performed without the sealing plate, and the ECC water discharge flow rate, the pressure loss coefficient of the fluidic device, and the discharge time of the air were evaluated for a reference. Then, the other test was performed after installing the sealing plate, and the above measured parameters were also evaluated and compared with the first test. The test conditions and results are summarized in Table I. When the initial conditions were satisfied, the ECC water started to be discharged by opening the quick opening valve installed downstream of the discharge pipe line and the data were logged on.

4.3 Experimental Results

The level change in the SIT was measured by the differential pressure transmitters. The discharge flow rate of the ECC water was deduced from the decreasing rate of SIT water level by Eq. (1):

$$W_{ECC}(t) = \rho_{ECC} A_{SIT} \frac{dh_{SIT}(t)}{dt} \cong \rho_{ECC} A_{SIT} \frac{h_{SIT}(t) - h_{SIT}(t+\triangle t)}{\triangle t} \quad (1)$$

The SIT water level decreased almost linearly regardless of the discharge flow rate. The instantaneous change rate of water level at time t could be approximated by first order differentiation (Eq. (1)) without causing a significant error in the evaluation of

the discharge flow rate. The discharge flow rate was calculated with a time difference of 2 seconds.

The discharge flow rate curves of two tests are shown in Fig. 6. The discharge flow rate decreased rapidly when the water level in the SIT dropped below the top of the stand pipe. The peak discharge flow rate of the ECC water was very similar to each other and the difference was sufficiently within the uncertainty band. The total duration of the ECC water discharge in the test without the sealing plate was about 3 seconds longer. This is due to the fact that the air discharge decreases the SIT pressure somewhat faster, resulting in a slight decrease of the ECC water discharge flow rate after the initiation of the air discharge.

Table 1 Summary of the test condition and results

	Test without sealing plate	Test with sealing plate
Initial SIT level (m)	7.98	7.94
Initial SIT pressure (kPa)	4,012	3,944
Peak flow rate (kg/s)	1,200	1,150
Duration of flow (sec)	88	85
FD K-factor*	11/120	12/120
Air discharge time (sec)	63	85

* large flow/small flow conditions

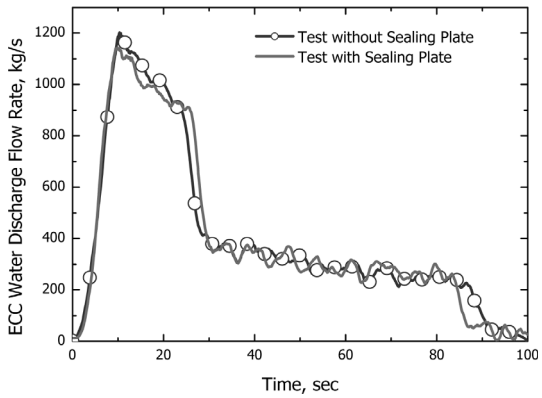

Fig. 6 Discharge flow rate of the ECC water from the SIT

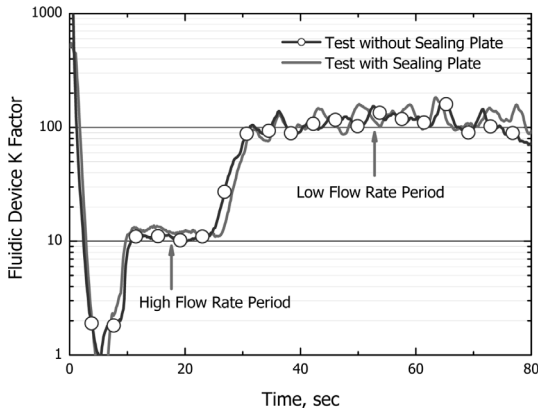

Fig. 7 Pressure loss coefficient of the fluidic device

The pressure loss coefficient of the fluidic device was determined by using Eq. (2), based on the pressure drop across the fluidic device:

$$K_{FD} = \triangle P_{FD} \frac{2}{\rho_{ECC} v_{ECC}^2} = \triangle P_{FD} \frac{2\rho_{ECC} A_{pipe}^2}{W_{ECC}^2} \tag{2}$$

The pressure loss coefficient of the fluidic device is shown in Fig. 7. The pressure loss coefficients of the fluidic device for two tests were very close to each other. Besides, almost a ten-fold higher pressure loss coefficient was achieved for the low flow rate period compared to the high flow rate period from whirling motion inside the vortex chamber.

The ECC water discharge flow rate can also be calculated in the following way by assuming that the SIT pressure change due to the ECC water discharge follows the polytropic process and the air behaves as an ideal gas:

$$(PV^{1.3})_{air,o} = (PV^{1.3})_{air,t} = (PV^{1.3})_{air,t+\triangle t} \tag{3}$$

$$\begin{aligned} Q_{ECC}(t) &= \left(\frac{dV}{dt}\right)_{air,t} \\ &\cong \frac{V_{air,t+\triangle t} - V_{air,t}}{\triangle t} \\ &= \left(P^{\frac{1}{1.3}} V\right)_{air,o} \frac{1}{\triangle t} \left[\left(\frac{1}{P}\right)_{air,t+\triangle t}^{\frac{1}{1.3}} - \left(\frac{1}{P}\right)_{air,t}^{\frac{1}{1.3}}\right] \end{aligned} \tag{4}$$

$$W_{ECC}(t) = \rho_{ECC} Q_{ECC}(t) \tag{5}$$

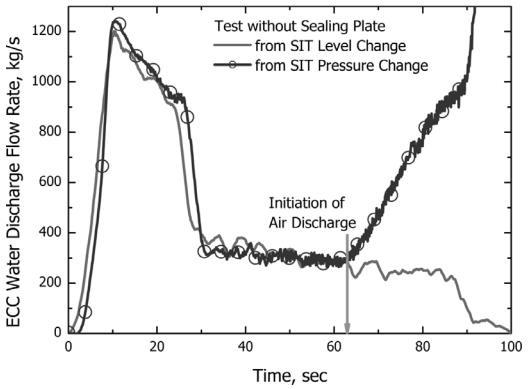

Fig. 8 Initiation of air discharge in the test without the passive sealing plate

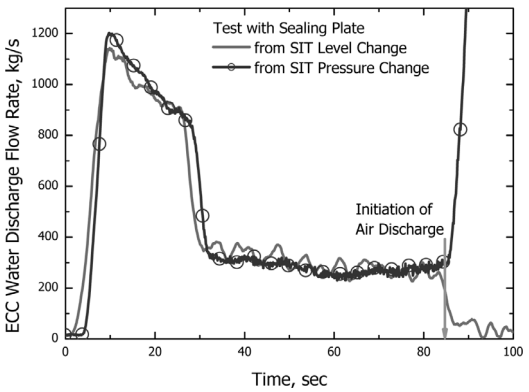

Fig. 9 Initiation of air discharge in the test with the passive sealing plate

The ECC water discharge flow rate obtained from Eq. (5) should be similar to the flow rate from Eq. (1) unless the total mass of the air is changed (i.e., before the air discharge is initiated). After the air discharge is initiated, the SIT pressure decreases not only due to the volume expansion of the air in the SIT but also due to the loss of the air mass resulted from the discharge. As a result, the ECC water discharge flow rate obtained from Eq. (5) starts to deviate from the discharge flow rate from Eq. (1) from the time of the initiation of the air discharge.

The ECC water discharge flow rates from Eqs. (1) and (5) are compared in Figs. 8 and 9 for the test without and with the sealing plate, respectively. The air discharge was initiated at the time of about 62 seconds in the test without the sealing plate. However, the air discharge through the stand pipe did not occur before the ECC water in the SIT was totally depleted in the test with the sealing plate. In addition, any noticible damage could be found on the sealing plate after the test.

5. Conclusions

A new device, passive sealing plate, was developed, which prevents the early nitrogen discharge through the stand pipe of the advanced SITs of evolutionary PWRs.

The performance of the sealing plate was evaluated using the VAPER test facility, equipped with a full-scale SIT. It was verified in the present tests that the passive sealing plate effectively prevented the air discharge through the stand pipe during the whole duration of the ECC water discharge. In addition, the major performance parameters of the advanced SIT such as the ECC water discharge flow rate, the duration of the ECC water discharge, the fluidic device K-factor were not changed with the installation of the sealing plate.

Acknowledgments

This work was financially supported by the Ministry of Knowledge Economy (MKE) of Korean Government.

References

1. Kim, I. S. and Kim, D. S., 2002, “APR1400 - Development Status and Design Features,” *Proc. ICAPP 2002, International Congress on Advances in Nuclear Power Plants*, Hollywood, Florida, June 9~13, 2002.
2. Song, C.-H., Kwon, T. S., Chu, I.-C., Jun, H. G. and Park, C. K., 2002, “Overview of Thermal Hydraulic Test Program for Evaluating or Verifying the Performance of New Design Features in APR1400 Reactor,” *Proc. ICAPP 2002, International Congress on Advances in Nuclear Power Plants*, Hollywood, Florida, June 9~13, 2002.
3. D. Thoma, 1928, “Vorrichtung zur Behinderung

des Ruchstromens," Deutsche Patentschrift No. 507-713.
4. T. Shiraishi, H. Watanabe, N. Nakamori and T. Sugizaki, 1994, "Characteristics of the Flow-Controlled Accumulator," *Nucl. Tech.,* Vol. 108, pp. 181-190.
5. T. Ichimura, S. Ueda, S. Saito and T. Ogino, 2000, "Design Verification of the Advanced Accumulator for the APWR in Japan," *Proc. ICONE 8, 8th International Conference on Nuclear Engineering*, Baltimore, MD, April 2~6, 2000.
6. I.-C. Chu, C.-H. Song, B. H. Cho and J. K. Park, 2008, "Development of Passive Flow Controlling Safety Injection Tank for APR1400," *Nucl. Eng. Des.,* Vol. 238, No. 1, pp. 200-206.